Structural Solutions and Seismic Resistance of Circular Columns by Steel Jacketing (Retrofitting)
Applied to Bridge Structures

Vanessa Amélia Manalo Alves (vanessa.alves1094@gmail.com)
IST - Technical University of Lisbon, Portugal, October 2019

Abstract: Earthquakes are catastrophic events that can cause significant material, economical and human damage. Bridges and viaducts are important structures that should keep working after an earthquake by accommodating deformation through ductility exploration. The most demanding elements are the pier ends, where, in the absence of seismic isolation system, energy dissipation occurs through the formation of plastic hinges. In some situations, some piers may need rehabilitation or retrofitting in order to replace or to increase the seismic resistance of the structure. In the present study advantages and inconveniences of concrete-filled steel tubes (CFST) or reinforced CFST (RCFST) subjected to seismic action are presented and, according to existing regulation codes and recommendations for this type of cross-section, a methodology is developed and implemented to take into account the nonlinear behavior of the plastic hinge on the seismic behavior of bridge piers. For the RC and the RCFST section, the M-N interaction curve and the moment-curvature (M-X) relation, for a certain axial load, were determined, considering concrete cracking effects. To reproduce the nonlinear behavior of the plastic hinge a nonlinear rotational spring was applied to the base of the pier, considering the moment rotation (M-θ) relation determined through the plastic hinge length. Time-History loads were applied to the structure, calibrated with the maximum acceleration value, determined for a certain value of a predefined behavior factor. After the linear and nonlinear analyses, a relation between the results was established to verify the ductility demands of the structure and correct attribution of the behavior factor.

Keywords: CFST, bridge, plastic hinge, ductility, seismic action, retrofitting

1. Introduction

An earthquake is an unpredictable natural catastrophe that occurs along the main discontinuities of the earths' crust, causing ground vibrations that should be considered for a safe and correct design of bridge and viaduct columns in countries with medium to high seismic activity which is the case of Portugal.

In 1995's Kobe earthquake noticeable infrastructure damage was caused, specially the collapse of bridges and viaducts which had a big impact in the surrounding area, as shown in **Figure 1.1**.

Figure 1.1-Colapse of the Hashin expressway due to Kobe earthquake (1995) [1].

1.1. Objectives and Methodology

Apart from literature revision on the use of Concrete-Filled Steel Tubes (CFST), regulations and recommendations were consulted in order to develop a methodology to determine the moment-curvature relation for a reinforced concrete section, designated as RC or BA, and a retrofitted RC section, designated as RCFST or BA-R. Based on that relation, the structure is modelled and through the application of base accelerations to the original and reinforced structures, a comparison between the behavior of both sections is made.

2. Seismic Analysis

2.1. European Norms: EN 1998-1 and EN 1998-2

The seismic analysis of bridge piers is extremely important to guarantee the requisites established by EC8-2 [2]:

i) Non collapse;

ii) Seismic damage limitation.

To study the seismic action on structures according to the analysis methods presented on **Table 2.1**, the seismic action must be characterized.

Table 2.1 - Seismic analysis methods.

Linear Analysis	Nonlinear Analysis
Linear static analysis	Nonlinear static analysis (*Pushover*)
Response spectrum method	Dynamic nonlinear analysis (*Time History*)

In linear analysis, strength, ductility and deformation criteria must be met. When considering works of art with ductile behavior, the elements subjected to plastic hinge formation must have enough bending stiffness to withhold the seismic action, as well as display shear and bending strength.

Seismic Action Characterization

The seismic action is characterized by three factors: the seismic type, seismic zone and source. Seismic action type 1 is known to have lower accelerations for low frequencies, causing a bigger impact, being the type of earthquake that caused the 1755 earthquake, in Lisbon. Seismic action type 2 presents higher accelerations for high frequencies. The seismic zone is used to evaluate the seismic action according to location. These seismic zones, soil types and maximum acceleration of reference for each seismic type can be consulted on the National Annex for the Portuguese mainland and islands on [3].

Importance factor

Bridges and viaducts are classified based on the post-earthquake damage impact. The higher the damage impact, the higher should be the importance factor of that structure.

Behavior factor

According to EN1998-1 [3], the behavior factor (q) is an approximation of the quotient between the seismic forces that the structure would be subjected to if it were to have a linear behavior and the forces that the structure is actually submitted. However, it's important to explore the inelastic deformation capacity and the energy dissipation capacity of structures subjected to seismic actions. This factor depends on the structure's ductility. The lower the value, the lower the ductility demands, leading to lower margin of exploration. There are two types of seismic behavior in bridges:

a) Ductile behavior: 1,50<q<3,5;

b) Limited ductility: q≤1,5.

The main objective of this work is to understand the behavior factor variation on a retrofitted structure through linear and nonlinear analysis, according to equation (2.1) and **Figure 2.1**.

$$q = M_{EL}/M_{NL} \quad (2.1)$$

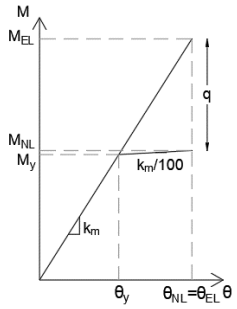

Figure 2.1-Graphic definition of the behavior factor (q).

2.2. Analysis Methods

To present the analysis methods there are some important seismic concepts to be explained.

Single degree of freedom (SDOF)

According to [4], when a system is reduced to a concentrated mass and there is only one displacement component, the structure is considered a single degree of freedom system, as illustrated on **Figure 2.2**.

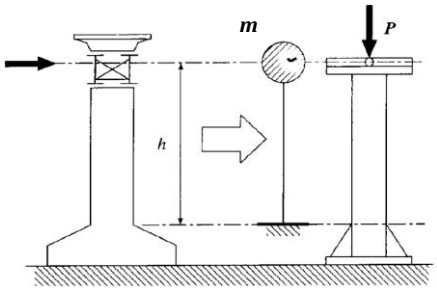

Figure 2.2-Single degree of freedom system

Dynamic Equilibrium Equation

The equation of motion for a SDOF is described by equation (2.2) [4].

$$m\ddot{q} + c\dot{q} + kq = Q(t) \quad (2.2)$$

Seismic action is consisted by ground movement and, therefore, base movement on structures. Displacements on a SDOF can be absolute or relative displacements, depending on which axis we want to consider as origin., in which the relative displacement is given by the difference between the base and free end displacements. The same theory is applied for velocity and acceleration, although for the latter, the relevant value is the absolute acceleration caused by the seismic action. It is then possible to write the equation of motion as presented on equation (2.3).

$$m\ddot{q}^* + c\dot{q}^* + kq^* = -m\ddot{q}_s(t) \equiv Q(t) \quad (2.3)$$

Plastic Hinge

A plastic hinge is considered to concentrate the nonlinear behavior along a finite length of an element. Since the pier base is the most affected area when the structure is subjected to seismic action, as shown on **Figure 2.3**, there is a plastification length (L_p) which is the distance from the first and last yielding section which can be simplified into a concentrated point.

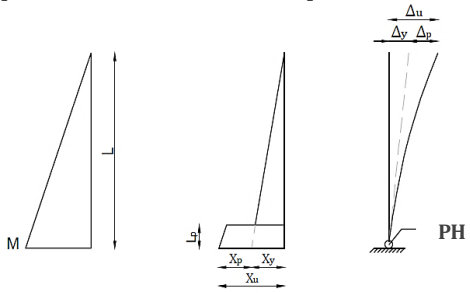

Figure 2.3-Plastic hinge concept, adapted from [2].

2.3. Time History Analysis

This type of analysis evaluates the structure's response with nonlinear behavior, subjected to a time dependent load which can be defined by a function. To determine the response of a structure subjected to a dynamic action, the step-by-step integration may be used. It's based on resolving the equation of motion in time steps. According to [5] the initial conditions of a time step should be the resulting conditions of the previous step, making each step a single linear analysis. This way, admitting material properties are constant between steps, it's possible to transform a nonlinear problem in a series of small enough steps of linear behavior.

3. Concrete-Filled Steel Tube (CFST)

The use of CFST joins the advantages of steel, which resists well in tension with high ductility, and concrete, which resists well in compression, being enhanced by the lateral confinement provided by the steel tube. The presence of concrete infill delays buckling modes and the outer steel delays the cracking and crushing of the concrete. These advantages are schematically illustrated in **Figure 3.1**. There is the possibility of maintaining the original RC structure, resulting in a Reinforced Concrete-Filled Steel Tube (RCFST), as shown by layers in **Figure 3.2**.

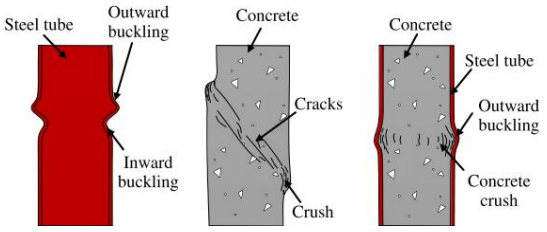

Figure 3.1-Colapse scheme of steel, RC and CFST sections, adapted from [6].

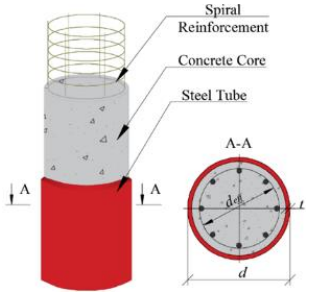

Figure 3.2-Layers of a RCFST [7].

3.1. Codes and Regulation

In this work, many codes and regulations were consulted:

i) European Norms: Eurocodes;

ii) American regulations: Bridge Design Manual (BDM) of the Washington State Department of Transportation (WSDOT) [8],

iii) Japanese norms: SRC Standard da Architectural Institute of Japan (AIJ) [9] and Design Specification for Highway Bridges – Part V Seismic Design from the Japan Road Association (JRA) [10];

iv) Other scientific papers and recommendations on CFST design.

3.2. Advantages and Disadvantages

According to Usami et al. [11], steel construction of bridge columns has been increasing due to fast and light construction, although these structures must be designed to resist strong earthquakes without collapse. Kitada [12] describes advantages of CFST such as the construction speed since the tubular steel section allows the exemption of formwork and rebars; cross-section reduction of the column when compared to RC columns due to the contribution of steel; increase of concrete strength due to confinement and therefore, steel buckling delay, as shown on **Figure 3.1**.

Table 3.1 presents the advantages and disadvantages of the CFST column system.

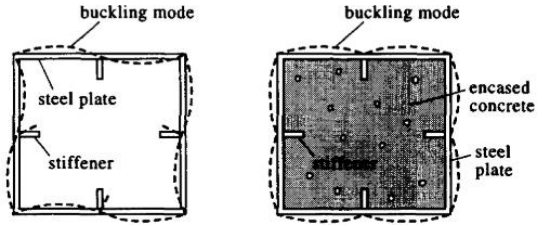

Figure 3.1-Buckling modes of steel and composite columns [12].

Table 3.1-Advantages and disadvantages of CFST.

Advantages	Disadvantages
•Fast execution; •Exemption of formwork; •Reduction of concrete shrinkage and creep; •Cross section reduction; •Lighter structure (vs RC); •Increased buckling resistance; •Increased capacity due to lateral confinement of concrete; •Reduction of the maximum displacement and residual drifts; •Global increase of ductility and load capacity; •Increase of energy dissipation capacity.	•Increase of cost (vs RC); •Complex column-to-foundation connections; •The infill concrete is not accessible or visible for quality control; •Limited specific design codes; •Lack of design recommendations.

Up to date there is no universal, adequate and less conservative regulation for designing these columns. In this sense, the specific study and design of column-to-foundation connections; evaluation of the optimal concrete infill height; consideration of bond between steel and concrete for the correct modelling and the correct seismic evaluation are necessary and must be deepened.

3.4. Column-to-Foundation Connections

In this connection there must be an efficient and economically accessible way of transferring demand strengths from the column to the foundation.

According to Hitaka [13] there are three types of connections used in Japan: **a)**base plate connection - oldest technique; **b)**encased base plate connection - its' use has been decreasing and **c)**embedded column connection which is the most used technique in bigger buildings.

4. Retrofitting

Dynamic analysis of existing structures is more complex when compared to new structures. Structural reinforcement may be needed when regulation codes become outdated and the structure doesn't verify the new code for safety; when deterioration of materials affects structural behavior; when damage is caused by accidental actions like seismic action and for prevention. In case of minor damage due to seismic action, structural reinforcement is the fastest and most economical solution opposing to the integral reconstruction of the element or structure. When it comes to important structures, such as viaducts, bridges and access ways, these must be safely accessible after an earthquake, which brings interest on reinforcement and rehabilitation of these types of structures.

4.1. European Norm: EN 1998-3

The third part of EC 8 [14] approaches the seismic evaluation and structural retrofitting of structures. The evaluation process of existing structures follows three main steps. Diagnosis is the determination of limit states, which define the functional demands after an earthquake and determine the safety level of the structure: 1) near collapse (NC); 2) significant damage (SD); and 3) damage limitation (DL). Security evaluation gathers information about the structure such as valid regulation on year of design and construction, definition of Knowledge Level and the respective Confidence Factor, which are presented in more detail on EN 1998-3 [14] and choice of linear or nonlinear analysis. At last, there is decision of intervention, which can be rehabilitation, reinforcement or no intervention, based on the safety evaluation and associated costs.

4.2. Types of Reinforcement

There are different types of reinforcement and the solution depends on the detected anomaly. In general, reinforcement techniques on columns are used to improve the behavior due to seismic action. They are based on jacketing with different materials such as steel, RC or CFRP layers and other composite materials. For RC columns, jacketing provides lateral confinement to the concrete, increasing its bending and shear capacity [12]. For tubular steel columns, the fastest solution is filling the void with concrete, creating a composite section which increases load capacity and ductility through the combined behavior of materials. Previous studies have shown that the

infill concrete height must follow the plastic hinge length since it's the most demanding area.

4.3. Previous Experimental Tests

Efficiency study on local steel jacketing of reinforced concrete columns

Cardoso et al. [15] carried out a study on representative specimen of the current column use in buildings. An incremental cyclic displacement was applied, and it was concluded that the steel jacketing originated better results than local bracing, noting that there was great increase on energy dissipation capacity, although 80% of that dissipation occurs for high levels of displacement, allied to loss of stiffness. Therefore, there should be a commitment between exploring energy dissipation capacity and stiffness degradation.

Seismic Retrofitting of Bridges in Japan

According to Unjoh et al [16] more than 3000 highway viaducts suffered damage with the Kanto earthquake in 1923. Due to the impact, all codes were reviewed and there was a great demand of column reinforcement. The most common types of reinforcement are the concrete infill and steel jacketing. On the latter, the interaction of materials must be guaranteed, specially at the base of the column, through anchor bolts and a layer of epoxy resin between both surfaces. The authors developed methods to define the priority of intervention on bridges and viaducts by applying cyclic loads to a RC column with a 1,6mm steel jacket and controlling the corresponding drift. Analyzing the hysteresis curves obtained for the original and retrofitted section, there is a noticeable increase of the peak resistance, as well as the energy dissipation capacity, leading to an improvement in ductility and bending strength.

Retrofitting of tubular steel columns

In this type of section retrofitting is made by partially or totally filling the tube with concrete or RC. Mamaghani [17] carried out experimental tests through pushover analysis comparing the results with numerical values for different heights of concrete infill, concluding that there are three main parameters considered to evaluate the strength capacity of the retrofitted columns: width-to-thickness relationship (4.1), slenderness (4.2) and the concrete infill height l_c.

$$R_t = \frac{d}{2t}\frac{\sigma_y}{E}\sqrt{3(1-\nu^2)} \qquad (4.1)$$

$$\bar{\lambda} = \frac{2h}{r}\frac{1}{\pi}\sqrt{\frac{\sigma_y}{E}} \qquad (4.2)$$

The author concludes that ductility is improved with the increase of the concrete height from $0{,}3L$ to $0{,}5L$ and deteriorates with the increase of slenderness and R_t parameter.

Influence of the jacket thickness in RC bridges

Olmos et al. [18] studied the influence of the jacket thickness through a pushover analysis of a RC column retrofitted solely on its base, considering a height of the plastic hinge length with a margin of 100 mm and different recommended values of retrofitting thickness [18]. It was concluded that the jacketing layer improves the base shear strength and ductility and that probability of the seismic demand being higher than resistant capacity decreases with the increase of the jacket thickness.

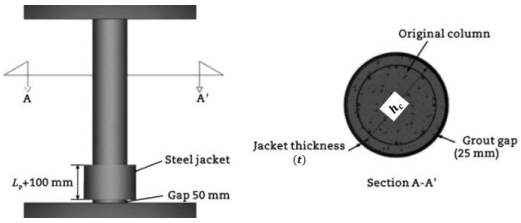

Figure 4.1-Retrofitted column, adapted from [18].

5. Load Capacity of sections

To evaluate the load capacity of a RC and retrofitted section, including the moment-curvature (M-χ) relation, a methodology was developed considering a generic circular RC section to be retrofitted by steel sheets.

5.1. Strength capacity under compound bending

Constitutive laws and geometric limitations

The adopted constitutive laws are the ones proposed by EN 1992 [19], as shown in **Figure 5.1** given by equation (5.1) for concrete, and in **Figure 5.2** given by equation (5.1) for reinforcing steel.

$$\sigma_c = \begin{cases} -f_{cd}\left[1-\left(1-\frac{\varepsilon_c}{\varepsilon_{c2}}\right)^n\right], 0 \le \varepsilon_c \le \varepsilon_{c2} \\ -f_{cd} \qquad\qquad , \varepsilon_{c2} \le \varepsilon_c \le \varepsilon_{cu2} \end{cases} \qquad (5.1)$$

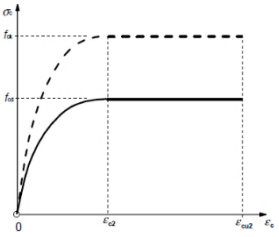

Figure 5.1-Parabola-rectangle diagram for concrete under compression [19].

$$\sigma_s = \begin{cases} -f_{yd} & ,\varepsilon_s \le -\varepsilon_y \\ E_s\varepsilon_s & ,-\varepsilon_y < \varepsilon_s < \varepsilon_y \\ f_{yd} & ,\varepsilon_s \ge \varepsilon_y \end{cases} \quad (5.2)$$

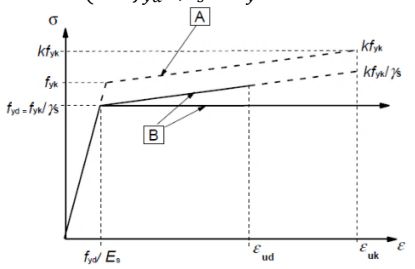

Figure 5.2-Stress-strain diagram for steel [19].

Where f_{cd} is the design value for concrete's compressive strength; f_{yd} is the design value for the yielding strength of steel; E is the modulus of elasticity; σ is stress; ε is strain and the subscripts c refer to concrete while s refers to steel and y refers to yielding.

Calculation method and simplified hypothesis

To calculate the strength capacity of a RC section, a study of maximum strain for each material is made based on the method presented on **Figure 5.3**.

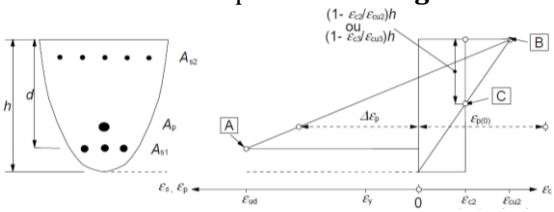

Figure 5.3-Admissible strain distribution [19].

In this work, the previous diagram was adapted to a RCFST section generally shown on **Figure 5.4**, where t_a is the thickness of the steel tube, h_a and h_c are the height of steel and concrete, respectively, c is the bar cover, and Φ is the reinforcing bar diameter.

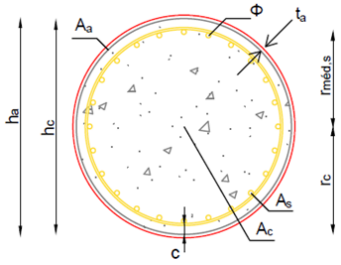

Figure 5.4-Generalized RCFST cross section.

For the strength capacity evaluation, the section was divided in n layers to which was determined the contribution of each material to calculate the applied forces for each layer. This is possible by defining the position of the neutral axis and correspondent curvature based on the fixation of a rotation point (A, B or C) allowing to determine the area, strain and correspondent stress and force, according to constitutive laws.

Adopted Simplifications:

- The admissible strain in compression is determined by the concrete (-3.5‰) and in tension is determined by the reinforcing rebars (10‰);
- Concrete doesn't resist to tension;
- Due to concrete confinement, the value of design stress is f_{cd};
- There is total bond between both materials;
- Bernoulli hypothesis is considered;
- The reinforcing rebars were simplified into a circular ring with a medium radius ($r_{med,s}$) and equivalent thickness (t_{eq}) obtained through simplifications that maintain the equivalent area of reinforcing steel;
- The section is divided into constant height layers;
- Considering all the simplifications made, the area in each layer is affected by a correction factor, defined by the quotient between the sum of all areas and the real cross-sectional area. Note that the more layers we have, the more refined is the study, in which f_c approximates to the unit.

RC Section

Figure 5.3 was adapted for a RC circular section, obtaining the stress-strain diagram presented on **Figure 5.5**.

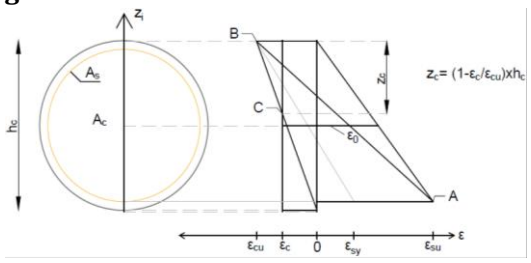

Figure 5.5-Admissible strain diagram for a RC section.

Rectangular parts of both materials were considered between each layer. To ease calculus work, a new reference origin was defined, which coincides with the geometric center of the section, stating that the compressive forces are related to negative strain values and tension forces are related to positive strain values as shown in **Figure 5.6**.

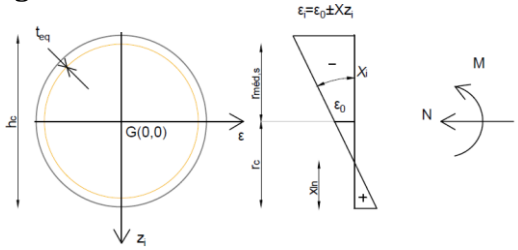

Figure 5.6-Reference axis definition for a RC section.

For a certain value of neutral axis height (x_{ln}), the corresponding curvature (χ) is known, knowing

therefore the strain in each layer, and consequently, the stress and force on each layer for each material. Finally, knowing the force of each material on each layer and the distance from the geometric center of the layer to the neutral axis position, it is possible to calculate the axial capacity and bending moment through equations (5.3) and (5.4), respectively.

$$N_{rd} = N_c + N_s = \sum A_{c,i} \times \sigma_{c,i} + \sum A_{s,i} \times \sigma_{s,i} \qquad (5.3)$$

$$N_{rd} = N_c + N_s = \sum A_{c,i} \times \sigma_{c,i} + \sum A_{s,i} \times \sigma_{s,i} \qquad (5.4)$$

Retrofitted Section

The methodology applied to the RC section was adapted to the retrofitted section by considering the joined actions of the RC core and the outer structural steel, obtaining the admissible strain diagram presented on **Figure 5.7**.

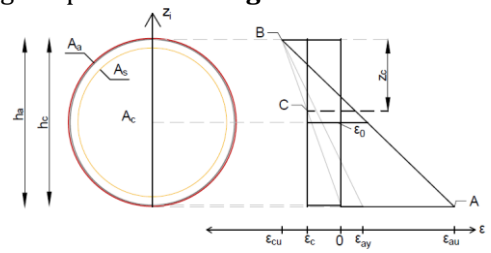

Figure 5.7-Admissible strain diagram for a RCFST section.

Through the same geometric simplifications, the new axis reference was defined as shown on **Figure 5.8**.

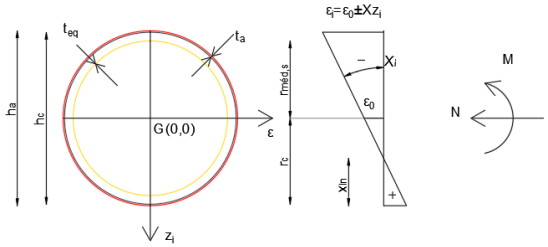

Figure 5.8-Reference axis definition for a RCFST section.

The equations to determine the axial force and bending moment have an additional element for the contribution of the structural steel as shown in equations (5.5) and (5.6).

$$N_{rd} = N_c + N_a + N_s \Leftrightarrow$$
$$N_{rd} = \sum A_{c,i} \times \sigma_{c,i} + \sum A_{s,i} \times \sigma_{s,i} + \sum A_{a,i} \times \sigma_{a,i} \qquad (5.5)$$

$$M_{rd} = M_c + M_a + M_s \Leftrightarrow$$
$$M_{rd} = \sum N_{c,i} \times z_{c,i} + \sum N_{s,i} \times z_{s,i} + \sum N_{a,i} \times z_{a,i} \qquad (5.6)$$

M-N interaction curve

The methodology presented in the previous section was implemented in an automatic program developed on Microsoft Excel (2019), allowing the user to determine the bending moment and axial values for many neutral axis heights. This way, an interaction curve, as shown for a generic RCFST section on **Figure 5.9**.

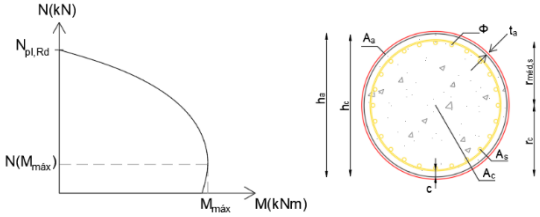

Figure 5.9-Bending moment-axial force (M-N) interaction curve for a generic RFCST section.

Notice that for works of art, the optimization area of this diagram corresponds to axial loads between 0,2N($M_{máx}$) and 0,4N($M_{máx}$).

5.2. Seismic capacity

Homogeneous section

To simplify calculations, both sections (RC and RCFST) were considered to have the same material: steel. Since the circular section presents a radial symmetry, any axis can be considered for this calculation, allowing that all inclined members were simplified into rectangular shapes to ease the inertia determination and further modelling properties.

Bending moment curvature relation (M-χ)

In a RC section, the M-χ can be defined by **Figure 5.10**, where Mcr is the bending moment for which the section starts cracking.

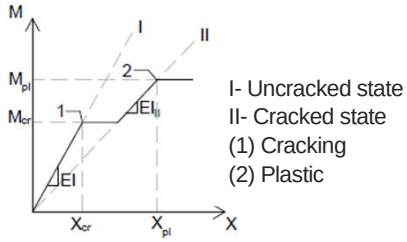

Figure 5.10-M- χ relation for a generic RC section.

For the composite section, three particular cases were considered leading to the generic diagram presented on **Figure 5.11**.

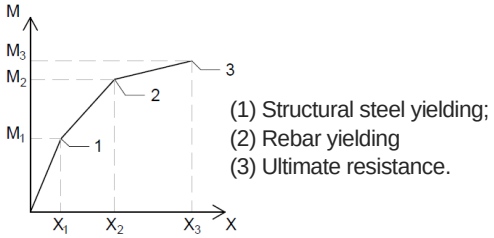

Figure 5.11-M- χ relation for a generic RCFST section.

Plastic Hinge simplification

This simplification is used to consider the nonlinear behavior and the incremental plastification of an element. In a simplified way, it is possible to determine the M-θ relation by

multiplying the M-χ by the plastic hinge length, later calibrating that value through equation (5.7).

$$L_p = 0{,}10L + 0{,}015 f_{yk} d_{bL} \quad (5.7)$$

6. Case Study

In the present section the structure modelling using SAP2000 software is approached, along with all the simplified hypothesis.

The case study is based on a real viaduct with three spans and a total length of 91,0 m as presented on **Figure 6.1**.

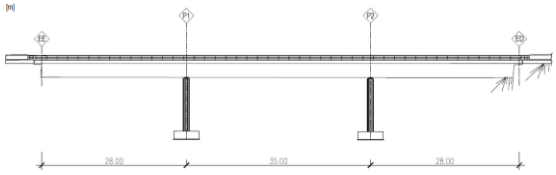

Figure 6.1-Side view of the viaduct.

The pier cross section is a RC column with 1,20m of diameter and 32Φ25 for rebars which is reinforced by a 10 mm tubular steel section, as illustrated on **Figure 6.2** for the original and reinforced section.

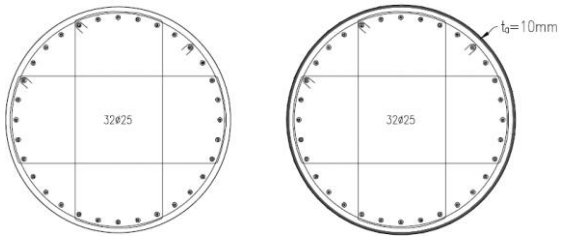

Figure 6.2-Original and reinforced cross section of the pier.

The materials and their characteristics are presented on **Table 6.1**.

Table 6.1-Material characteristics.

C30/37		A500		S355	
$\Upsilon_c\ [kNm^3]$	25,0	$\Upsilon_s\ [kNm^3]$	78,5	$\Upsilon_s\ [kNm^3]$	78,5
$E_c\ [GPa]$	33,0	$E_s\ [GPa]$	200,0	$E_a\ [GPa]$	210,0
$f_{cd}\ [MPa]$	20,0	$f_{yd}\ [MPa]$	435,0	$f_{yd}\ [MPa]$	275,0
$f_{ck}\ [MPa]$	30,0	$f_{yk}\ [MPa]$	500,0	$f_{yk}\ [MPa]$	275,0
$f_{ctm}\ [MPa]$	2,9	$f_{su}\ [MPa]$	435,0	$f_{su}\ [MPa]$	275,0
ε_{co} [‰]	2,00	ε_{sy} [‰]	2,18	ε_{sy} [‰]	1,31
ε_{cu1} [‰]	3,50	ε_{su1} [‰]	10,00	ε_{su1} [‰]	10,00

6.1. Model definition

After defining materials, the section was defined through a homogeneous material.

The structure was simulated as a single degree of freedom system with a concentrated mass at the free end of the cantilever. **Figure 6.3** presents the cross section of the bridge board at mid span. Based on that cross section, the mass was calculated considering an increase of 25% to account for the cross-section variation to the support area and the mass of the girders, resulting in 959,4 ton.

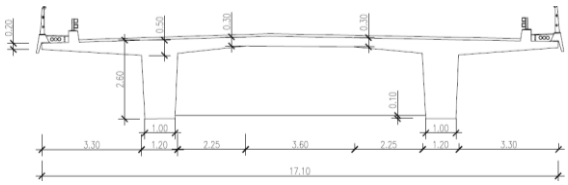

Figure 6.3-Midspan deck cross section.

Through the methodology presented on the previous section, the cross section of the pier was divided into 50 layers of constant height, resulting in the bending moment-axial force interaction diagrams presented on **Figure 6.4**.

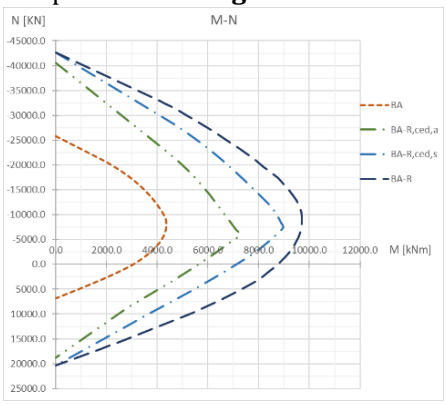

Figure 6.4-M-N interaction diagrams for the original and reinforced sections.

The maximum values of axial force and bending moment are presented on **Table 6.2**.

Table 6.2-Maximum values of M-N for the original and reinforced sections.

	$M_{max}\ (kNm)$	$N_{max}\ (kN)$
BA	4370	25797
BA-R	9715	42635

Seismic Capacity

For a constant axial load, given by the pier reaction, the bending moment-curvature (M-χ) relation was determined, resulting on the diagrams illustrated on **Figure 6.5** and **Figure 6.6**.

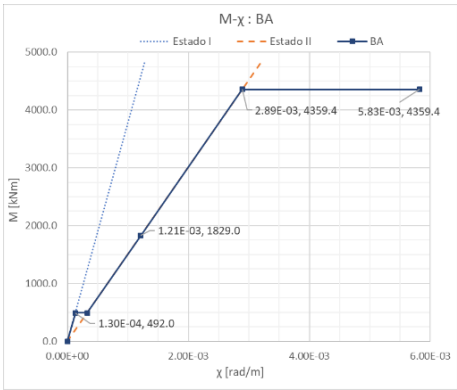

Figure 6.5- M-χ relation for the RC section.

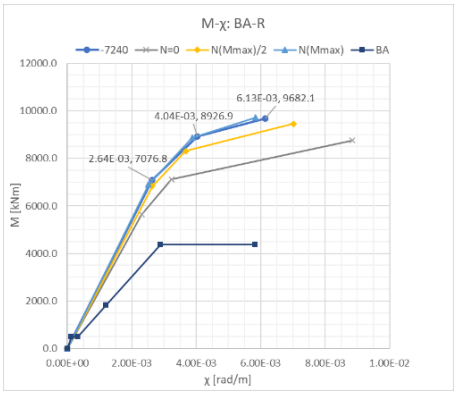

Figure 6.6-M-χ relation for the RC and RCFST sections.

Moment-rotation relation (M- θ)

Based on the moment-curvature relation, it's possible to obtain the moment-rotation relation by multiplying the values of curvature by the plastic hinge length, obtaining the values presented on **Figure 6.7**.

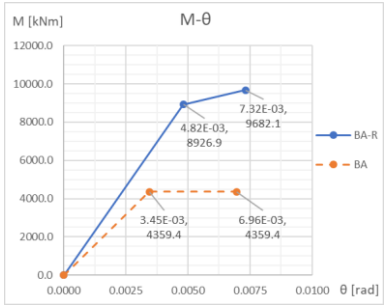

Figure 6.7-M-θ relation for the RC and RCFST sections.

In the linear elastic model, the spring stiffness is given by the quotient between the moment and rotation of the yielding point. For the nonlinear analysis, the plastic hinge is given by the nonlinear behavior through the complete definition of the M-θ, considering that the second part of the diagram as horizontal after yielding point.

Time History Analysis

To analyze the original structure, time history base accelerations were applied to the base of the structure. Ten signals, determined for a maximum acceleration of $1m/s^2$ given by the method presented on [20] were considered. To adapt these values, determined with time steps of 0.01 seconds with a total duration of 40 seconds, a constant value was determined to linearly affect the signals. This is possible by knowing the fundamental period of the structure, the definition of response spectrum and by defining a value of behavior factor (q=2). With the fundamental period value, the corresponding acceleration value can be determined through the average of the accelerations consulted in the elastic response spectrum for the previous signals, as shown in **Figure 6.8**.

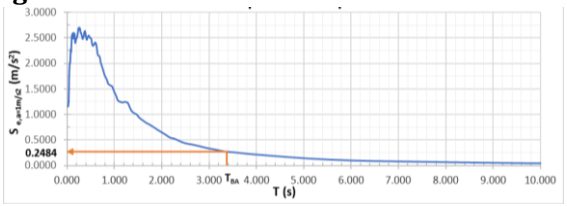

Figure 6.8-Average of the accelerations determined for a maximum acceleration of $1m/s^2$.

On the other hand, the maximum bending moment can be determined through the M-N interaction diagram for the constant axial load on the pier, as presented on **Figure 6.9**.

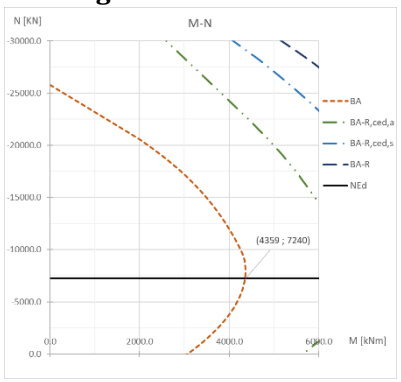

Figure 6.9-Maximum bending moment for a constant axial load, N_{Ed}.

For this value, it's possible to define the value of the constant (C) through the definition of design response spectrum and the elastic response spectrum given by equations (6.1) and (6.2), resulting on equation (6.3).

$$S_e = S_d \times q \tag{6.1}$$

$$S_e = C \times \bar{S}_{e,a=1m/s^2} \tag{6.2}$$

$$S_d \times q = C \times \bar{S}_{e,a=\frac{1m}{s^2}} \Leftrightarrow C = \frac{S_d \times q}{\bar{S}_{e,a=\frac{1m}{s^2}}} \Leftrightarrow \Leftrightarrow C = \frac{0{,}4545 \times 2}{0{,}2484} = 3{,}658 \tag{6.3}$$

After running 10 base acceleration history cases, assuming zero initial conditions of displacement and acceleration for linear and nonlinear analyses

the M-θ relation was obtained. This relation for one time history analysis is illustrated on **Figure 6.10** and **Figure 6.11**.

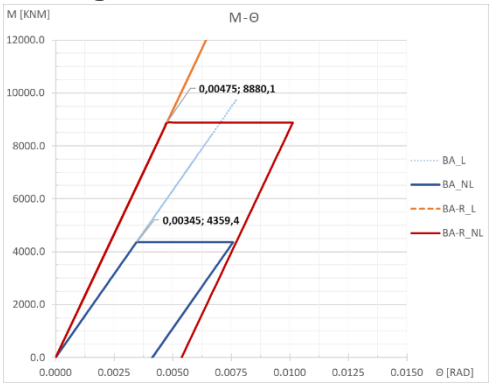

Figure 6.10-M-θ relation for the RC and RCFST sections.

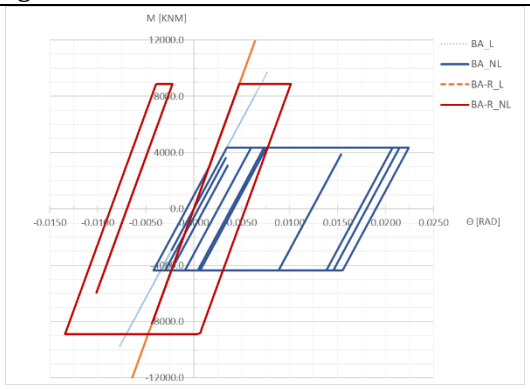

Figure 6.11-M-θ relation for the RC and RCFST sections after one time history analysis.

To better understand the contribution of the number of signals used in a study, the results were analyzed for 5 and 10 signals, resulting on the behavior factors presented on **Table 6.3** and **Table 6.4**.

Table 6.3-Behavior factor for the RC section.

	BA: $\bar{M}_{max}$ (kNm)		
	EL	**NL**	**q**
5 signals	9185,6	4359,4	2,11
10 signals	9430,0	4359,4	2,16

Table 6.4- Behavior factor for the RC section

	BA − R: $\bar{M}_{max}$ (kNm)		
	EL	**NL**	**q**
5 signals	13841,7	8880,1	1,56
10 signals	13496,0	8880,1	1,52

It is concluded:

- There is a reduction for the behavior factor value determined for the reinforced section;
- The M-N interaction diagram increased, leading to an increase of axial load and bending moment capacity;
- The rotation at the base is significantly reduced by 60% from the original section;
- The results obtained from the average of 5 and 10 signals were similar.

7. Final Remarks and Conclusions

It is concluded that:

- The combined behavior of both materials is favorable since the structural steel improves confinement to the concrete and the concrete increases the buckling resistance;
- In new construction, steel replaces the use for formworks;
- To improve the adhesion between materials, modifications may be made to increase the area of contact;
- The ultimate resistance obtained for a CFST is higher than the joined resistances of the circular tubular and RC section;
- There is a global increase of resistance, ductility and energy dissipation capacity;
- There is an increase of cost when compared to regular RC sections, although the pier cost has a small impact on the global cost of the work of art.
- The lack for regulations may be contoured by adapting existing regulations for steel, reinforced concrete and composite structures.

Future research

The use of this type of column system has great potential and needs further development.

- An adequate regulation and recommendation for design should be developed;
- Modelling the real M-θ relation should be used, which can be obtained by experimental tests;
- The adhesion between materials should be considered;
- When retrofitting an element, it is also important to evaluate the new capacity of the structure if the behavior factor is to be maintained.

References

[1] H. Ghasemi, H. Otsuka, J. D. Cooper, and H. Nakajima, "Aftermath of The Kobe Earthquake," 1996. [Online]. Available: https://www.fhwa.dot.gov/publications/publicroads/96fall/p96au17.cfm. [Accessed: 03-Jan-2019].

[2] CEN, *EN 1998-2 Eurocode 8: Design of structures for earthquake resistance – Part 2: Bridges*, vol. 2, no. 22. 2010.

[3] C. 115 (LNEC), *Eurocódigo 8: Projecto de estruturas para resistência aos sismos*. 2009, pp. 1–226.

[4] J. J. R. T. Azevedo and J. M. S. F. M. Proença, *Dinâmica de Estruturas*. 1991.

[5] R. W. Clough and J. Penzien, "Response to General Dynamic Loading: Step-by-Step Methods," in *Dynamics of Structures*, Third., CSI Computers & Structures, Inc., 2003, pp. 111–132.

[6] L. H. Han, W. Li, and R. Bjorhovde, "Developments and advanced applications of concrete-filled steel tubular (CFST) structures: Members," *J. Constr. Steel Res.*, vol. 100, pp. 211–228, 2014.

[7] A. L. Krishan, E. A. Troshkina, and M. A. Astafyeva, "Strength of Short Concrete Filled Steel Tube Columns with Spiral Reinforcement," *IOP Conf. Ser. Mater. Sci. Eng.*, vol. 262, no. 1, 2017.

[8] WSDOT-Washington State Department of Transportation, *Bridge Design Manual (LRFD)*. 2017.

[9] A. I. of J. (AIJ), *Standard for Structural Calculation of Steel Reinforced Concrete Structures*. 1987, p. 104.

[10] J.R.Association, "Design Specifications for Highway Bridges, Part V Seismic Design," 2002.

[11] B. T. Usami, "Ductility of Concrete-Filled Steel Box Columns Under Cyclic Loading," vol. 120, no. 7, pp. 2021–2040, 1994.

[12] T. Kitada, "Ultimate strength and ductility of state-of-the-art concrete-filled steel bridge piers in Japan," *Eng. Struct.*, vol. 20, no. 97, pp. 347–354, 1998.

[13] T. Hitaka, K. Suita, and M. Kato, "CFT Column Base Design and Practice in Japan," 2003.

[14] CEN, *EN 1998-3 Eurocode 8: Design of structures for earthquake resistance - Part 3: Assessment and retrofitting of buildings*, vol. 1. 2010.

[15] A. Cardoso, J. Appleton, and S. P. Santos, "Análise da eficiência da técnica de encamisamento localizado na reparação ou reforço de pilares de betão armado com recurso a chapas de aço ou manta de fibras de carbono," pp. 1–8, 2004.

[16] S. Unjoh, T. Terayama, Y. Adachi, and J. Hoshikuma, "Seismic retrofit of existing highway bridges in Japan," *Cem. Concr. Compos.*, vol. 22, no. 1, pp. 1–16, 2000.

[17] I. H. P. Mamaghani, "Seismic Design and Retrofit of thin-walled steel tubular columns," *13th World Conf. Earthq. Eng.*, no. 271, 2004.

[18] B. Olmos, J. M. Jara, G. Gómez, and G. Martínez, "Influence of steel jacket thickness on the RC bridges' seismic vulnerability," *J. Traffic Transp. Eng. (English Ed.*, vol. 6, no. 1, pp. 15–34, 2019.

[19] CEN, *EN 1992-1-1 Eurocode 2: Design of concrete structures - Part 1-1: General rules for buildings*. 2004.

[20] L. Guerreiro, "Ação Sísmica - Apontamentos da disciplina de Engenharia Sísmica de Pontes do Mestrado de Engenharia de Estruturas," 2011.